NASA TECHNICAL MEMORANDUM

NASA TM X-2856

NASA TM X-2856

FLYOVER AND STATIC TESTS TO STUDY FLIGHT VELOCITY EFFECTS ON JET NOISE OF SUPPRESSED AND UNSUPPRESSED PLUG NOZZLE CONFIGURATIONS

by Roger Chamberlin

Lewis Research Center
Cleveland, Ohio 44135

NATIONAL AERONAUTICS AND SPACE ADMINISTRATION • WASHINGTON, D. C. • AUGUST 1973

Page Intentionally Left Blank

1. Report No. NASA TM X-2856	2. Government Accession No.	3. Recipient's Catalog No.
4. Title and Subtitle FLYOVER AND STATIC TESTS TO STUDY FLIGHT VELOCITY EFFECTS ON JET NOISE OF SUPPRESSED AND UNSUPPRESSED PLUG NOZZLE CONFIGURATIONS		5. Report Date August 1973 6. Performing Organization Code
7. Author(s) Roger Chamberlin		8. Performing Organization Report No. E-7186 10. Work Unit No. 501-24
9. Performing Organization Name and Address Lewis Research Center National Aeronautics and Space Administration Cleveland, Ohio 44135		11. Contract or Grant No. 13. Type of Report and Period Covered Technical Memorandum
12. Sponsoring Agency Name and Address National Aeronautics and Space Administration Washington, D.C. 20546		14. Sponsoring Agency Code
15. Supplementary Notes		

16. Abstract

Two spoke-type suppressor plug nozzles and a basic plug nozzle were tested for noise and thrust performance. The nozzles were mounted on an underwing nacelle on an F-106B aircraft, and tests were made both statically and in flyovers at Mach 0.4 at an altitude of 91 meters (300 ft). The flight and static data were adjusted to common reference conditions so that direct comparisons could be made. The noise characteristics that these nozzles would have on a large multiengine aircraft at a 640-meter (2100-ft) sideline distance are also presented. Flight noise levels for all three nozzles were higher than static at comparable conditions; and a shift in the frequency spectra was seen from static to flight, indicating the presence of a forward velocity effect on the noise characteristics.

17. Key Words (Suggested by Author(s))	18. Distribution Statement
Flight test; Plug nozzle; Noise suppression; Suppressor nozzle; Flyby noise characteristic; Static noise characteristic	Unclassified - unlimited

19. Security Classif. (of this report)	20. Security Classif. (of this page)	21. No. of Pages	22. Price*
Unclassified	Unclassified	33	$3.00

* For sale by the National Technical Information Service, Springfield, Virginia 22151

FLYOVER AND STATIC TESTS TO STUDY FLIGHT VELOCITY EFFECTS ON JET NOISE OF SUPPRESSED AND UNSUPPRESSED PLUG NOZZLE CONFIGURATIONS

by Roger Chamberlin

Lewis Research Center

SUMMARY

Two spoke-type suppressor plug nozzles and a basic plug nozzle were tested for noise and thrust performance. The nozzles were mounted on an underwing nacelle on a modified F-106B aircraft, and tests were made both statically and in flyovers at Mach 0.4 at an altitude of 91 meters (300 ft). The flight and static data were adjusted to common reference conditions so that direct comparisons could be made. The noise characteristics that these nozzles would have on a large multiengine aircraft at a 640-meter (2100-ft) sideline distance are also presented.

The two suppressor nozzles reduced the noise levels relative to the basic plug nozzle over most of the frequency range but at the expense of thrust losses. Flight noise levels for all three nozzles were higher than static at comparable conditions; and a shift in the frequency spectra was seen from static to flight, indicating the presence of a forward velocity effect on the noise characteristics. At the large-multiengine sideline condition, the 32-spoke suppressor did show some additional noise reduction, relative to the basic plug, as might be expected; but the 64-spoke suppressor did not.

INTRODUCTION

Keeping the community noise level down to an acceptable level is one of the major problems that will be incurred by advanced transport aircraft. During takeoff and climbout the primary source of noise is the jet exhaust. Much work is being done on many different types of suppressors in an attempt to reduce the jet noise. However, the vast majority of this work is done on static test facilities, and there are effects that result from the aircraft being in flight. In an actual flight situation, external air is passing over the suppressor. Most of the suppressors being tested work on the prin-

ciple of breaking up the jet into smaller segments. Breaking up the jet shifts the frequencies higher and increases the mixing with the surrounding air. This mixing process could be changed by external air flowing over the nozzle to the jet. Also the mechanics of a moving noise source are not fully understood and the so-called dynamic effect on amplitude (ref. 1) (in addition to Doppler effects on frequency) that results can change the jet noise considerably.

The Lewis Research Center is investigating the noise characteristics of various suppressed and unsuppressed nozzles both statically and in flight (refs. 2 and 3). The flight tests are conducted with an F-106B aircraft modified to carry two J85-GE-13 afterburning turbojet engines in aft underwing nacelles (fig. 1). The flight acoustic data are obtained with the aircraft flying directly overhead at an altitude of 91 meters (300 ft) and at a Mach number of 0.4. The static acoustic data are taken on a radius of 30 meters (100 ft) from the exhaust nozzle. Nozzle thrust performance is also obtained both on the ground and in flight with an onboard thrust measuring system (ref. 4).

Three nozzles were tested in this particular study, a plug nozzle with rounded-tip plug and two spoke-type suppressors, one with 32 spokes and one with 64 spokes. The suppressors were built around the plug and, in concept, would be storable inside the plug cavity. Independent noise measurements and analysis were made, and the results are reported in reference 1.

A mathematical program was developed to adjust the flyby acoustic data to static conditions at 30 meters (100 ft) (ref. 3), so that comparisons could be made between flight and static noise levels. The flight data were also extrapolated out to a 640-meter (2100-ft) sideline and scaled up to four large engines (approx. 266 893-newton (60 000-lbf) thrust) (refs. 5 and 6). Comparisons are also made at these conditions.

SYMBOLS

A_{E8}	nozzle effective throat area (hot), cm^2 ($in.^2$)
D	sum of nacelle and nozzle external pressure and skin friction drags, N (lbf)
EPNL	effective perceived noise level, EPNdB
F	nozzle gross thrust, N (lbf)
$F_{i,p}$	ideal thrust of primary jet, N (lbf)
$(F - D)/F_{i,p}$	nozzle gross thrust coefficient
f	frequency, Hz
M_0	free-stream Mach number

PNL	perceived noise level, PNdB
P_8	total pressure at primary nozzle throat station, N/m^2 abs (psia)
P_8/p_0	nozzle pressure ratio
p_0	free-stream static pressure, N/m^2 abs (psia)
R	radius of plug at station 600.25 (236.32), 10.65 cm (4.19 in.)
r	radial distance from plug centerline, cm (in.)
SPL	sound pressure level, dB
T_8	total temperature at nozzle throat, K (^oR)
V_{ac}	aircraft velocity, m/sec (ft/sec)
V_j	jet velocity, m/sec (ft/sec)
V_R	relative velocity, $V_j - V_{ac}$, m/sec (ft/sec)
X	axial distance from station 600.25 (236.32) to plug tip, 25.40 cm (10.00 in.)
x	axial distance aft, starting from station 600.25 (236.32), cm (in.)
θ	acoustic angle, measured from exhaust centerline
ω	ratio of secondary to primary weight flow
$\omega\sqrt{\tau}$	corrected secondary weight flow
τ	ratio of secondary to primary total temperature

APPARATUS

Installation

Details of the airplane modifications and the nacelle-engine assembly are given in references 7 and 8. A schematic of the research nacelle and the rounded-tip plug nozzle is shown in figure 2. The nacelle was located at the 32-percent semispan with a downward incidence of 4.5^o (relative to the wing chord) so that the aft portion of the nacelle was tangent to the aft wing lower surface. The nacelle was positioned parallel to the aircraft centerline and in such a way as to provide approximately 0.64-centimeter (0.25-in.) clearance at the wing trailing edge. Details of the wing modifications, nacelle shape, and mounting strut are given in reference 8. The strut with the wide fairing described in reference 8 was used.

The gas generator was a J85-GE-13 turbojet engine with afterburner. The variable-area nozzle was removed and replaced with a fixed plug nozzle. The plug loads were

taken out through three struts. For the flight tests the nacelles had normal shock inlets with blunted cowl lips. Secondary cooling air was supplied from the inlet and metered at the periphery of the compressor face by a calibrated rotary valve. For the static tests the normal shock inlet was replaced with a bell-mouthed inlet, and the secondary cooling air was supplied from an external source.

Test Hardware

The three nozzles tested are shown in figures 3 to 5. Detailed dimensions of the plug nozzle assembly are given in reference 9, and dimensions of the rounded tip are given in figure 6. The conical primary flap had a 17° half-angle, and the shroud used was the one labeled $x/l = -0.08$ in reference 9. Details of the two spoke suppressor nozzles are given in figures 7 and 8. In addition to having a different number of spokes, the suppressors had different spoke shapes. The spokes for the 32-spoke nozzle were a V-gutter triangle shape (fig. 8) and resulted in rectangular flow areas. The geometry of the spokes on the 64-spoke configuration was rectangular and resulted in triangular flow areas. For the suppressor nozzles the throat is moved from a point near the maximum plug diameter, aft to the plane of the spokes. The throat area was fixed at 710 square centimeters (110 $in.^2$), which restricted engine operation to military and part power. The restricted engine operation limited the plug temperature to 1006 K (1810° R), thereby eliminating any plug cooling requirements.

Thrust Measurements

A load-cell technique (ref. 4) was used to measure the thrust minus drag on the nozzle and nacelle in order to determine exhaust nozzle performance both statically and in flight. As shown in figure 2, the nacelles were supported by two attachment links with a strain-gage, load-cell assembly located between the links. The front and rear links were each attached to the wing and nacelle with fittings having low-friction bearings. Each link was installed so that a line through the axis of rotation of the upper and lower bearings was perpendicular to the nacelle thrust axis. This system of links transfers only the loads parallel to the nacelle axis to the load cell. Accelerometers in the nacelle provide corrections for axial weight components and acceleration effects.

Engine airflow was determined by using prior engine calibration data (ref. 10) along with in-flight measurements of engine speed, pressure, and temperature at the compressor face. Knowing compressor inlet flow, total pressure and temperature at the turbine discharge, and fuel flow rates, enabled us to obtain other parameters at the

primary nozzle exit, such as effective area A_{E8}, total pressure P_8, and total temperature T_8, from previous calibrations. An onboard digital data system recorded pressures, temperatures, and load-cell output on magnetic tape.

Noise Measurements

The microphones used for both the static and flyover tests were 2.54-centimeter (1-in.) diameter ceramic type. Their frequency response was flat to within ±2 dB (decibels ref. 0.0002 μ bar) for grazing incidence over the frequency range used (50 to 10 000 Hz). The output of the microphones was recorded on a two-channel direct-record tape recorder. The entire system was calibrated for sound level in the field before and after each test with a conventional discrete calibrator.

Both the flyover and static signals were recorded on magnetic tape. The tape was played back through 1/3-octave-band filters and then reduced to digital form. The averaging time for data reduction was 0.1 second for the flyover data and a small portion of the static data. The major portion of the static data was reduced with 0.125-second averaging time. Meteorological conditions, in terms of dry-bulb and dewpoint temperatures, wind velocity and direction, and barometric pressure, were recorded periodically throughout the tests. Wind speeds were less than 10 knots during all tests.

PROCEDURE

All the testing was done at Selfridge Air National Guard Base in Mount Clemens, Michigan. A layout of the field is shown in figure 9. The flyover path was 45.72 meters (150 ft) east of and parallel to the main runway. The static tests were conducted at one of the two areas shown, depending on the local activity in either area.

Flyover Tests

Aircraft altitude during the flyover was determined by using an onboard radio altimeter and a barometric altimeter, along with ground-based radar. A calibrated nose boom was used to determine free-stream static and total pressure, aircraft angle of attack, and yaw angle. Aircraft velocity was obtained from a Mach meter.

Noise measurements were taken with a microphone 1.2 meters (4 ft) off the ground over a concrete surface and directly under the flightpath of the aircraft (fig. 10). The microphone was fitted with a wind screen. A second (backup) microphone was positioned on the concrete surface. Both microphones were set up to receive the acoustic pressure

waves at grazing incidence.

The flyover tests were made at an altitude of 91 meters (300 ft) and at a Mach number of 0.4. These flight conditions were picked because they are typical of a large-transport takeoff profile near the maximum noise position. These conditions are also consistent with the safe operation of the F-106 aircraft, and good repeatable data could be obtained. At 91-meter (300-ft) altitude and Mach 0.4 the data were repeatable to within ±1.5 PNdB.

While the aircraft was flying overhead and while the noise data were being recorded, the main engine of the F-106, a J75, was at idle power and the unused J85 research engine was windmilling. The J85 engine with the test nozzle was operated over a range of power settings. When the aircraft was in the overhead position, a 400-hertz signal was put on the tape by an observer on the ground. After the tests were completed, the research J85 was shut off and allowed to windmill, and several passes were made with the J75 at idle power to assure that background noise levels were sufficiently low (10 dB or more below the test levels recorded).

Static Tests

The static noise measurements were made on a 30-meter (100-ft) radius over concrete using a microphone 1.2 meters (4.0 ft) off the ground (fig. 11). For the 32-spoke suppressor, data were recorded at acoustic angles θ between 20° and 50°. For the 64-spoke suppressor and the basic plug, data were recorded only at the angle of peak noise. The microphone was pointed at the noise source to receive the acoustic pressure waves at normal incidence. As for the flyover tests the microphone was fitted with a wind screen. While the noise measurements were being taken, the main engine (J75) was at idle power with the variable nozzle open. It was necessary to run the J75 to provide electrical power to the J85 engines and to run the data system. The J85 engine with the test nozzle was run over a range of power settings and the second J85 engine was shut down. After the tests on the research nozzle were complete, the research engine was also shut down; and noise measurements were taken with only the J75 running at idle power to determine J75 and background noise levels.

Data Reduction

The basic noise data, flyby and static, were adjusted to a standard day of 298.15 K (537° R) and 70-percent relative humidity using the simplified procedure of Federal Aviation Regulation (FAR) 36 (ref. 6). The data were also adjusted to free-field conditions. Details of these adjustments are given in reference 3. In order to determine if

any forward velocity effects were present, a comparison was made of the flyby and static data. The static data were adjusted to free-field, standard-day conditions and also to account for the differences of the acoustic pressure waves meeting the microphone at normal incidence instead of grazing. The flyby noise data were adjusted to free-field, standard-day conditions and to a 30-meter (100-ft) distance, and the Doppler frequency shift was accounted for.

In order to examine the noise suppression characteristics that these nozzles would have on a large multiengine aircraft, a third adjustment was made to the flyby data. The flight data were adjusted for a typical four-engine aircraft at standard-day conditions as measured on a 640-meter (2100-ft) sideline by a 1.2-meter (4.0-ft) high microphone. Details of these adjustments are given in references 5 and 6.

During the flyover, the direct ray distance from the nozzles to the microphone continuously changes. The angle between the direct ray and the jet exit centerline, referred to as the acoustic angle, also changes. The acoustic angle is shown in figure 12. Also shown in figure 12 is the distance of the true path of the sound and the ground distance between the aircraft and microphone, for different values of acoustic angle.

Some additional corrections to the flyby data of the 64-spoke suppressor were necessary. Some interference was picked up on the tape in a band of frequencies from approximately 2600 to 4000 hertz. Corrections in this frequency range were made using the frequency spectra from the data reported in reference 1. The reference 1 data were recorded at the same time but on an independent system. Data comparisons for the other nozzles and for the 64-spoke suppressor at static conditions showed excellent agreement.

RESULTS AND DISCUSSION

Basic Results Flight and Static Tests

The flyover perceived noise levels directly under the flightpath are shown in figure 13 for all three nozzles. Also the effective perceived noise levels for these profiles are listed. The basic plug nozzle, which has no suppression devices, produced the highest noise level and has a relatively flat profile. Both suppressor nozzles show a reduction in peak noise level and a slightly steeper profile, which reduces the duration time. The peak noise of the basic plug is spread over a wide range of angles from 45° to 65°, whereas the suppressor nozzles show the noise dropping off more sharply after the peak. However, the reduction in effective perceived noise level (EPNL) is about the same as the reduction in peak perceived noise level (PNL). So the change in duration has little benefit at these conditions.

The effect of relative velocity on the perceived noise and effective perceived noise, in flight, is shown in figure 14. The basic plug nozzle has the highest noise levels over the whole range of relative velocity. The noise levels, both PNL and EPNL, drop off with varying powers of the velocity. At lower relative velocities the effect of velocity changes on the noise becomes less and less. At high relative velocities the noise (PNL) produced by the basic plug is proportional to approximately $(V_R)^{6.0}$ and drops off to $\sim(V_R)^{3.5}$ and down to $\sim(V_R)^{1.0}$ as relative velocity is lowered. Both suppressor nozzles are even less sensitive to velocity changes, showing a proportionality of approximately $(V_R)^{2.8}$ at high relative velocities and an increase in noise with decreasing velocity at lower velocities. In this low-relative-velocity region the effect of velocity is extremely small and noise produced by jet scrubbing against the spokes probably becomes dominant. This effect is seen on all three nozzles. The noise levels of the basic plug and the 32-spoke suppressor nozzle are considerably higher (10 PNdB or more) than the background noise of the basic aircraft. Therefore, the background noise could not have significantly influenced these data.

Figure 15 shows the frequency spectra at the flyby peak PNL points for all the three nozzles. The 64-spoke suppressor shows a reduction over the entire frequency range and the 32-spoke suppressor shows reductions over the whole range, except at the very high frequencies. Segmented nozzles such as these increase the mixing of the jet with surrounding air and reduce the noise levels at all frequencies. However, the segmented nozzles change the jet from one large jet to many small jets, and in so doing they create proportionally more high-frequency noise. The spoke suppressors show the largest noise reduction at the low frequencies, and this reduction drops off with increasing frequency.

Values of peak perceived noise taken statically are shown in figure 16. These data were adjusted to free-field, standard-day conditions, the same as the flight data. The effect of changing relative velocity is much more uniform at static conditions. Statically, all three nozzles are much more sensitive to velocity changes. The noise of the basic plug nozzle is proportional to approximately $(V_R)^{6.5}$ over the entire velocity range tested. The noise of the 32-spoke suppressor nozzle varies with approximately $(V_R)^{5.2}$ over the entire range. Only the 64-spoke suppressor shows any apparent change in proportionality, going from approximately $(V_R)^{7.2}$ at high velocities to $(V_R)^{2.7}$ at lower velocities. When the effects of relative velocity from static to flight conditions are compared (figs. 14 and 16), two effects are seen. With a moving noise source in flight, the dependency on velocity is much less; and as relative velocity is reduced, this effect becomes still smaller. These two effects are much more evident on the two suppressor nozzles than on the unsuppressed basic plug nozzle.

The frequency spectra for the static peak perceived noise points are shown in figure 17. As in flight, the 64-spoke suppressor shows reduction over the entire frequency range; and the 32-spoke suppressor also shows reduction over the entire range, except

for the very high frequencies. The general shapes of the curves statically are different from those in flight. This result is discussed in the next section, but it can be pointed out here that statically the noise suppression is greater at the higher frequencies and less at the lower frequencies, whereas in flight there was less suppression at the high frequencies and more at the low.

In addition to noise characteristics, nozzle thrust performance must also be taken into consideration. Nozzle performance as a function of nozzle pressure ratio is shown in figure 18. Performance for both static and flyby is presented in the form of nozzle gross thrust coefficient, defined as measured thrust-minus-drag ratioed to the ideal thrust of the primary jet. Plug nozzles are good performance nozzles; the basic plug has peak gross thrust coefficients of 0.983 statically and 0.943 in flight. The drop in performance in flight is probably caused by drag on the primary flap and losses on the plug body. The 32-spoke suppressor gave peak gross thrust coefficients of 0.897 statically and 0.840 in flight; and the 64-spoke suppressor, 0.750 statically and 0.725 in flight. The drop in performance of the suppressor nozzles in flight is caused by the drag on the large base area of the spokes. The 32-spoke suppressor shows more scatter at low pressure ratios and more sensitivity to pressure ratio, probably because of the shape of the spokes. The spokes for this nozzle are a V-gutter shape (fig. 8), which directs the flow into an aerodynamic throat just aft of the spokes. This aerodynamic throat and the performance of the nozzle are sensitive to pressure ratio and external flow over the nozzle.

For a realistic comparison of the suppressor nozzles, both the noise reduction and the nozzle performance should be compared together. This comparison is made in figure 19. Peak noise reduction (ΔPNdB) is plotted against thrust loss, with the basic plug as the reference for both noise and performance. The flyby data for the two suppressors and the reference basic plug are adjusted to a nozzle pressure ratio of 2.4 and a relative velocity of 543 meters per second (1780 ft/sec). The static data for all three nozzles are adjusted to a nozzle pressure ratio of 2.0 and a relative velocity of 600 meters per second (1970 ft/sec). When comparing static data and flight data for either nozzle, it must be kept in mind that the basic plug values also change from static to flight. The 32-spoke suppressor gave more noise suppression per percent loss in thrust. The 64-spoke suppressor, although it has good suppression, has large thrust losses. Some refinement could be made to these nozzles to improve the ventilation of the base area of the spokes and thus reduce the base drag and improve the performance. Also these nozzles were tested at low pressure ratios (statically, $P_8/p_0 \approx 2.0$; flyby, $p_8/p_0 < 2.5$), and the performance should improve at high pressure ratios.

Comparison of Flight and Static Noise Test Results

All the static data were recorded on a 30-meter (100-ft) radius with the aircraft stationary. The flight data were recorded with the aircraft moving at Mach 0.4 at an altitude of 91 meters (300 ft). In order to make a legitimate comparison between static and flight data, these differences must be eliminated. Whenever direct comparisons are made here between flight and static, the data from both have been adjusted to a common reference condition, which is free field and standard day on a 30-meter (100-ft) radius. The adjustments made to both the static and flight data have been discussed previously.

Figure 20 shows a comparison of flight and static perceived noise levels for the 32-spoke suppressor with all data at the reference condition. The comparison is made at relative velocities for static and flight of 503 and 518 meters per second (1650 and 1700 ft/sec), respectively. This difference in relative velocities would cause differences of less than 1 PNdB. The flyby noise levels are higher at all angles, indicating a flight velocity effect on the noise characteristics of this nozzle.

The frequency spectra at each of the four comparable angles are compared in figure 21. The adjusted flyby data at frequencies below 160 hertz and above 5000 hertz are somewhat questionable. At frequencies below 160 hertz, the short integration time (0.1 sec), the rapidly changing conditions of the flyover, and the narrowness of the frequency bands combine to give results that are not reliable. At frequencies above 5000 hertz, the acoustic signal received at the ground station quite possibly is below the noise floor of the recording equipment (ref. 11). Values of the atmospheric absorption coefficient are very large at these high frequencies and multiply the noise floor to unrealistically high noise levels when the adjustment is made for atmospheric absorption and distance. Both flight and static spectra change with acoustic angle; this effect is discussed in connection with figures 25 and 26. At the higher angles the static spectra exhibit a dip at or near 1600 hertz. This dip is caused by a specific ground reflection that was not accounted for. The major difference that appears at all angles is that there is more high-frequency noise and less low-frequency noise in flight. This could be a result of increased mixing in flight. The increased mixing with the small segmented jets would increase high-frequency noise and would help dissipate the large coalesced jet which produces the low-frequency noise. Also of possible influence and not discussed herein is the "dynamic effect" on amplitude that results from a moving noise source.

The static and flight perceived noise levels at the reference condition for the basic plug and the 64-spoke suppressor are compared in figure 22. Static data are not available for these nozzles at different angles. The basic plug is approximately 5.5 PNdB noisier in flight than static, and the 64-spoke suppressor is approximately 4.0 PNdB noisier in flight than static.

The frequency spectra for the basic plug are compared in figure 23. The overall perceived noise levels compared in figure 22 are adjusted to the same relative velocity; however, the frequency spectra in figure 23 are compared at different relative velocities. The static data were taken at a relative velocity of 600 meters per second (1970 ft/sec), and the flight data at 558 meters per second (1831 ft/sec). Had these data been taken at a common relative velocity, the differences at the high frequencies would be greater than shown and those at the low frequencies would be less than shown. Again there is a dip in the static spectra near 1600 hertz that is caused by a ground reflection. The differences in the spectra here are similar to those obtained with the 32-spoke suppressor. The flight data appear to indicate increased mixing, resulting in more high-frequency noise and less low-frequency noise, which yields a higher perceived noise level.

The same comparison is made for the 64-spoke suppressor in figure 24. The different relative velocities are similar to that of the basic plug, and the differences in the two spectra are similar to those for the other two nozzles.

In addition to changes in the noise going from static to flight, there are also changes in the frequency spectra with acoustic angle. These changes with acoustic angle are seen both statically and in flight. A comparison of static frequency spectra at different acoustic angles is shown in figure 25 for the 32-spoke nozzle. At high frequencies the levels are similar for all angles. At low frequencies there is a definite shift in the spectra. At low angles, there is much more low-frequency noise close to the jet axis; and as the angle or the distance from the jet axis is increased, the low-frequency levels drop off. The reason could be that the noise is generated along the length of the jet, rather than from a point source. The low-frequency noise is generated several diameters downstream of the nozzle exit, after the small jets have coalesced into one. As the microphone is moved closer to the jet axis, even though it is along a radius, it is closer to the location where the low-frequency noise is generated; and therefore the low frequency levels recorded are higher.

Flight frequency spectra at different angles are shown for the 32-spoke suppressor in figure 26. The data have been adjusted to the reference conditions so they can be compared with each other. The low frequencies show the same trends as the static data, but this is in a range (below 160 Hz) where the flight data are questionable. At higher frequencies in a range from 800 to 5000 hertz, the trend is toward increasing noise at higher angles. This trend could also be caused by the noise being generated over the length of the jet instead of at a point source. This effect may be geometry sensitive because, although it is recognizable on the other nozzles, it was not as prevalent.

Predicted Sound Levels for a Large Multiengine Aircraft

The data presented in this section are equivalent to noise levels, measured by a

1.2-meter (4.0-ft) high microphone over a concrete surface at a 640-meter (2100-ft) sideline distance, of a large four-engine (266 893-N (60 000-lbf) thrust per engine) aircraft flying by at a 304.8-meter (1000-ft) altitude at Mach 0.4 on a standard day. These data were obtained by taking the flyby data shown in figure 13 and making the necessary adjustments for engine size, number of engines, aircraft altitude, and sideline condition.

The perceived noise levels at these conditions as a function of acoustic angle are shown for all three nozzles in figure 27. The suppressors still show significant reductions from the unsuppressed plug nozzle, but the results for the two suppressors are closer at these conditions. The reason is the attenuation of the high-frequency noise over the long distances to the sideline. The suppressor nozzles, as was discussed previously, produce mostly high-frequency noise. In figure 27 the 32-spoke suppressor is seen to have a shorter duration time (time between the points 10 dB down from the peak) than the other nozzles. So the 32-spoke suppressor will show an additional reduction of EPNL beyond what results from lowering the peak perceived noise level. This effect can be seen in figures 30 and 31.

Figure 28 shows values of perceived noise level and effective perceived noise level as a function of relative velocity. At these conditions the perceived noise is more sensitive to changes in relative velocity than the basic flyby data under the flightpath. Again, the relative difference in noise level drops as relative velocity decreases. The basic-plug noise level is proportional to $(V_R)^{7.50}$, which drops to $(V_R)^{4.66}$ and to $(V_R)^{0.50}$ at the lowest velocity. The 32-spoke-suppressor noise level is proportional to $(V_R)^{4.38}$ at high velocities and drops to $(V_R)^{0.53}$ before increasing at very low velocities. The 64-spoke-suppressor noise level is proportional to $(V_R)^{3.04}$ and drops to $(V_R)^{1.70}$ at lower velocities. In general, the noise levels are proportional to much higher powers of velocity here (at the 640-m (2100-ft) sideline) than directly under the flightpath in a flyby. The values of EPNL follow the same trends as the values of PNL.

The frequency spectra for all three nozzles at or near the peak perceived noise point are shown in figure 29. As can be seen, much of the high-frequency noise has been attenuated by the atmosphere. Because the high-frequency levels are now much lower, the low-frequency values contribute proportionally more to the perceived noise level. The two suppressors have similar noise levels at the low frequencies, and the differences at the high frequencies are not as significant now because the sound pressure levels at these frequencies are lower. Thus, there is less difference in perceived noise level between the two suppressors relative to the flyby condition. The basic plug had high noise levels at the low frequencies compared to the suppressors, and these differences are still present at the scaled sideline condition. However, the basic plug had high noise levels at the high frequencies also, which are now attenuated. So there is still a significant difference in the overall perceived noise level between the basic plug and the suppressors, but the suppressors do not show any large additional reduc-

tion in perceived noise level at the scaled sideline condition.

Figure 30 is a plot of reduction in effective perceived noise as a function of thrust loss at the scaled sideline conditions. The 32-spoke suppressor shows an increase in suppression when compared to perceived noise levels at the F-106 - J85 flyby conditions. The 64-spoke suppressor shows no increased suppression. Figure 31 shows a breakdown of the noise suppression associated with the different operations. Figure 31(a) shows, for the 32-spoke suppressor, a loss in suppression when engine size is scaled up, then a large increase in suppression going to the sideline distance, and a further increase when duration is taken into account. The same breakdown for the 64-spoke suppressor is shown in figure 31(b). For both nozzles an increase in noise reduction is achieved by going to a sideline distance, but large losses in noise reduction result from scaling up to large engines.

SUMMARY OF RESULTS

Two suppressor nozzles, a 32 spoke and a 64 spoke, and an unsuppressed plug nozzle were tested for noise and performance both statically and in flight. The nozzles were mounted on a J85-GE-13 afterburning turbojet engine installed under the wing of an F-106B aircraft. Static acoustic data were taken on a 30-meter (100-ft) radius, and flight data were taken with the aircraft flying by at a 91-meter (300-ft) altitude and a speed of Mach 0.4. The following results were obtained:

1. Both suppressor nozzles reduced the noise level relative to the unsuppressed nozzle but at the expense of relatively large thrust losses.

2. When the flyby data were adjusted to static conditions on a 30-meter (100-ft) radius, all three nozzles showed higher noise levels from the flight data, indicating the presence of a flight velocity effect on the noise.

3. The suppressor nozzles reduced the noise over a major portion of the frequency spectrum. However, statically there was more suppression at the high frequencies, and in flight there was more suppression at the low frequencies.

4. Adjusting the flyby data to a large multiengine aircraft at sideline conditions increased the noise reduction of the 32-spoke suppressor.

5. At low values of relative velocity, in flight the suppressor nozzles showed an increase in noise with decreasing relative velocity.

Lewis Research Center,
National Aeronautics and Space Administration,
Cleveland, Ohio, May 15, 1973,
501-24.

REFERENCES

1. Brausch, J. F.: Flight Velocity Influence on Jet Noise of Conical Ejector, Annular Plug and Segmented Suppressor Nozzles. General Electric Co. (NASA CR-120961), Aug. 1972.

2. Burley, Richard R.; and Karabinus, Raymond J.: Flyover and Static Tests to Investigate External Flow Effect on Jet Noise for Non-Suppressor and Suppressor Exhaust Nozzles. Paper 73-190, AIAA, Jan. 1973.

3. Burley, Richard R.; Karabinus, Raymond J.; and Freedman, Robert J.: Flight Investigation of Acoustic and Thrust Characteristics of Several Exhaust Nozzles Installed on Underwing Nacelles on an F106 Airplane. TM X-2854, 1973.

4. Groth, Harold W.; Samanich, Nick E.; and Blumenthal, Philip Z.: Inflight Thrust Measuring System for Underwing Nacelles Installed on a Modified F-106 Aircraft. NASA TM X-2356, 1971.

5. Anon.: Jet Noise Prediction. Aerospace Information Report 876, SAE, July 10, 1965.

6. Anon.: Federal Aviation Regulations, Vol. III, Part 36, Noise Standards: Aircraft Type Certification, Dept. of Transportation, Federal Aviation Administration, Washington, D.C.

7. Crabs, Clifford C.; Mikkelson, Daniel C.; and Boyer, Earle O.: An Inflight Investigation of Airframe Effects on Propulsion System Performance at Transonic Speeds. Presented at the 13th Annual Symposium of the Society of Experimental Test Pilots, Los Angeles, Calif., Sept. 25-27, 1969.

8. Mikkelson, Daniel C.; and Head, Verlon L.: Flight Investigation of Airframe Installation Effects on a Variable Flap Ejector Nozzle of an Underwing Engine Nacelle at Mach Numbers from 0.5 to 1.3. NASA TM X-2010, 1970.

9. Samanich, Nick E.; and Chamberlin, Roger: Flight Investigation of Installation Effects on a Plug Nozzle Installed on an Underwing Nacelle. NASA TM X-2295, July 1971.

10. Antl, Robert J.; and Burley, Richard R.: Steady-State Airflow and Afterburning Performance Characteristics of Four J85-GE-13 Turbojet Engines. NASA TM X-1742, 1969.

11. Little, John W.; Miller, Robert L.; Oncley, Paul B.; and Panko, Raymond E.: Studies of Atmospheric Attenuation of Noise. NASA Acoustically Treated Nacelle Program. NASA SP-220, 1969, pp. 125-135.

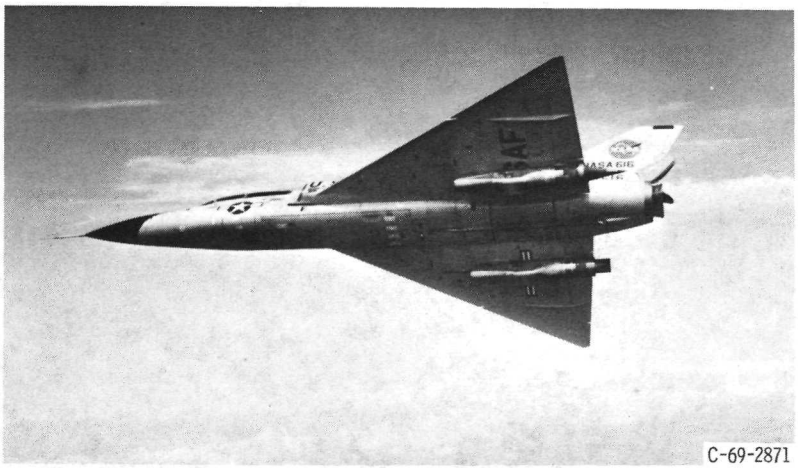

Figure 1. - Modified F-106B aircraft in flight.

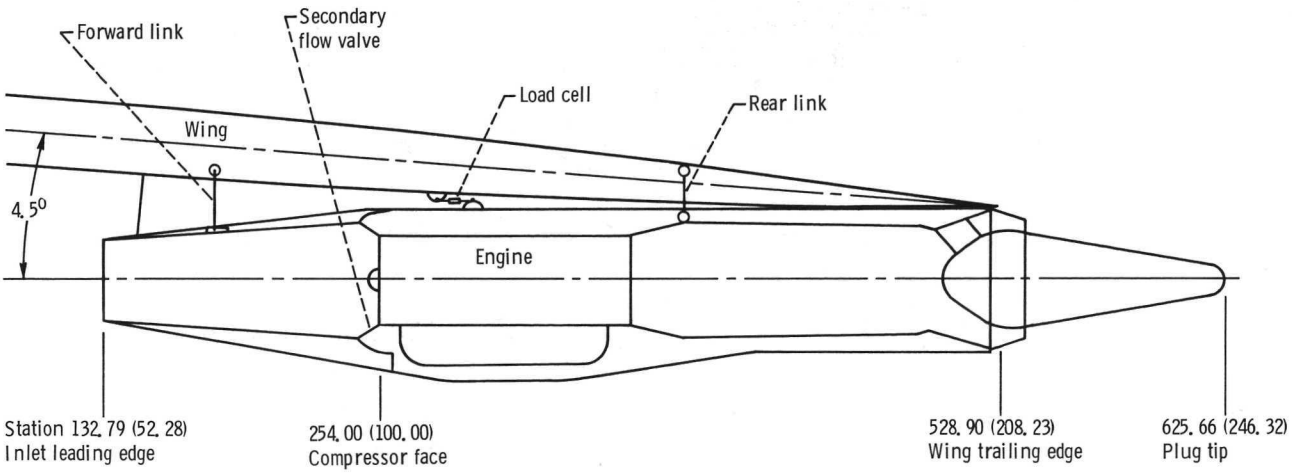

Figure 2. - Schematic of nozzle installation. (All dimensions are in cm (in.).)

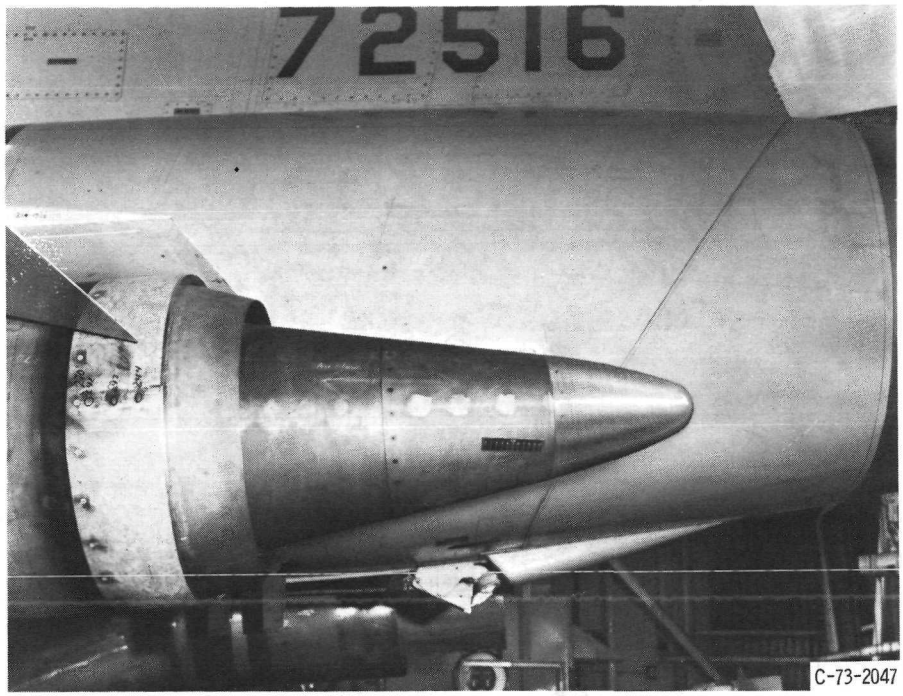

Figure 3. - Basic plug nozzle.

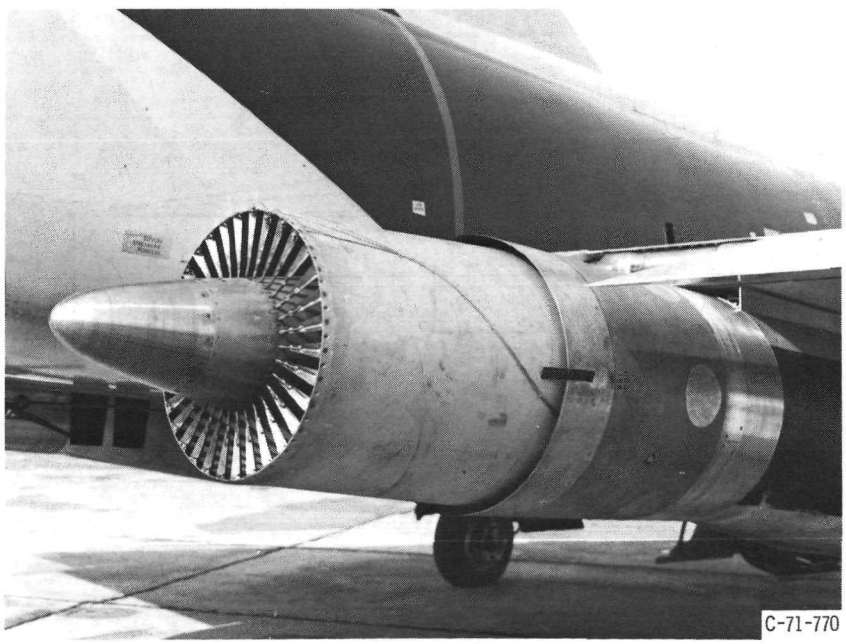

Figure 4. - Thirty-two-spoke suppressor nozzle.

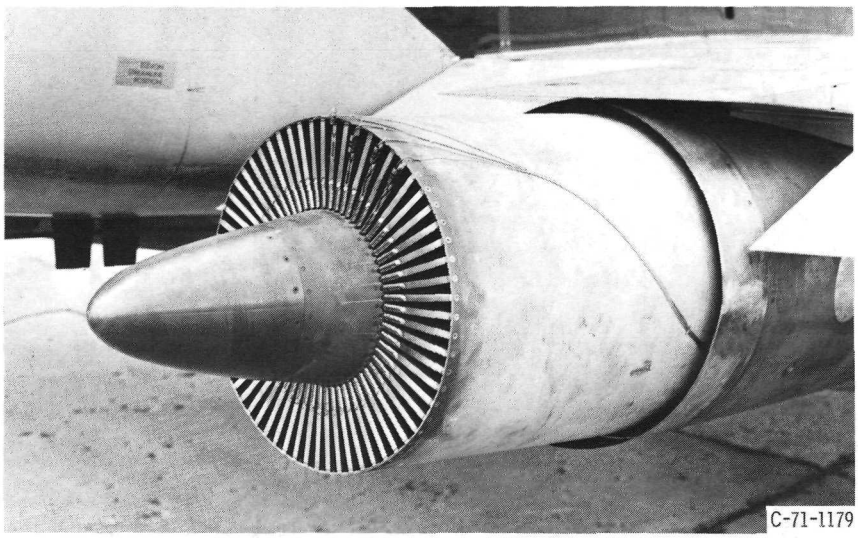

Figure 5. - Sixty-four-spoke suppressor nozzle.

x/X	r/R
0	1.00
.10	.95
.20	.90
.30	.85
.40	.79
.50	.73
.60	.66
.70	.58
.80	.49
.90	.34
.95	.24
1.00	0

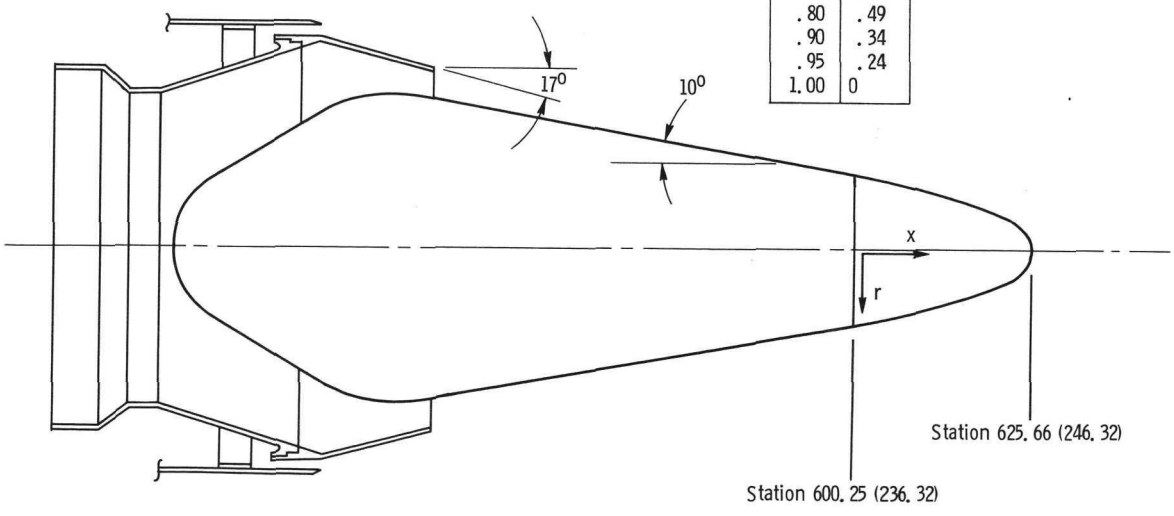

Figure 6. - Basic plug nozzle geometry. (All dimensions are in cm (in.).) Axial distance from station 600.25 (236.32) to plug tip, X = 25.40 cm (10.00 in.); radius of plug at station 600.25 (236.32), R = 10.65 cm (4.19 in.).

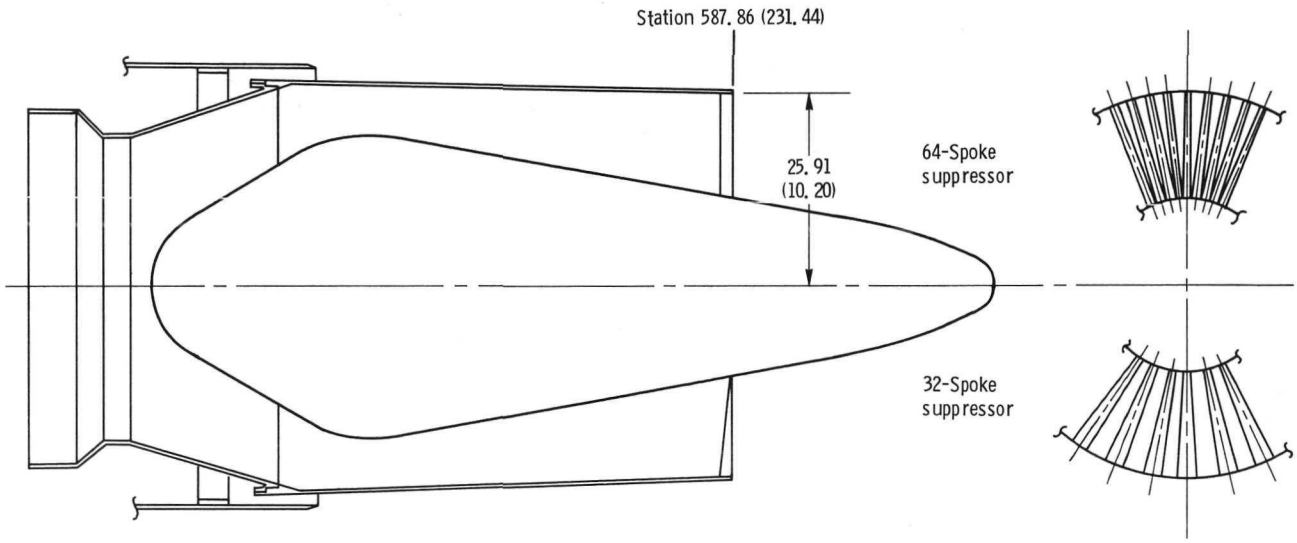

Figure 7. - Spoke nozzle geometries. (All dimensions are in cm (in.).)

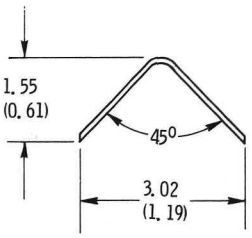

Section A-A

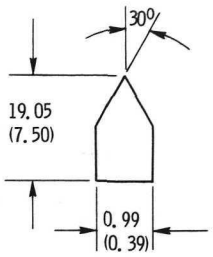

Section B-B

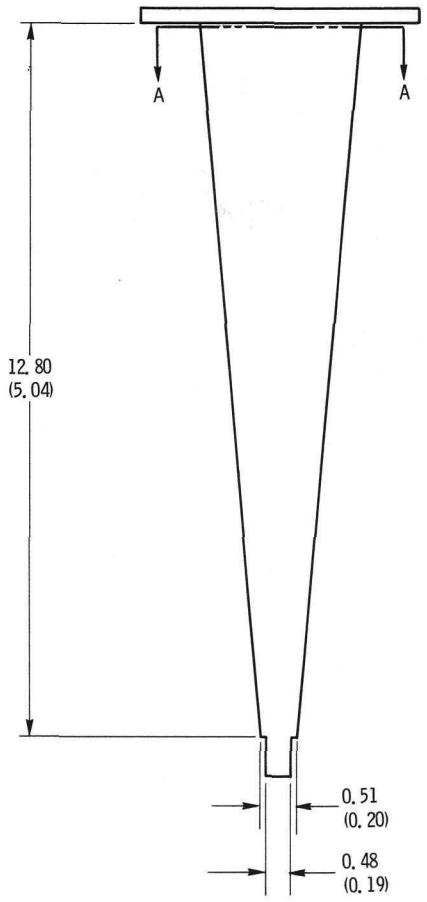

Spoke design for 32-spoke configuration

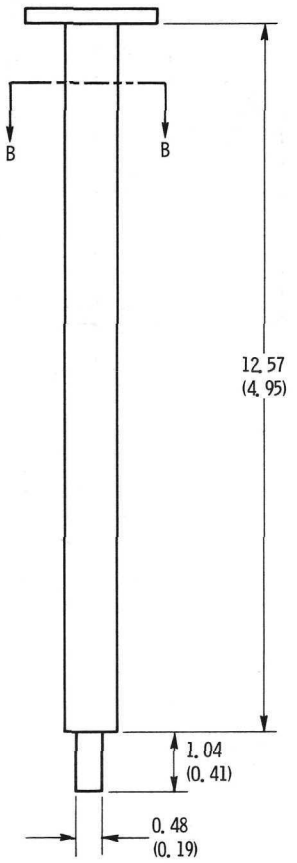

Spoke design for 64-spoke configuration

Figure 8. - Spoke geometries. (All dimensions are in cm (in.).)

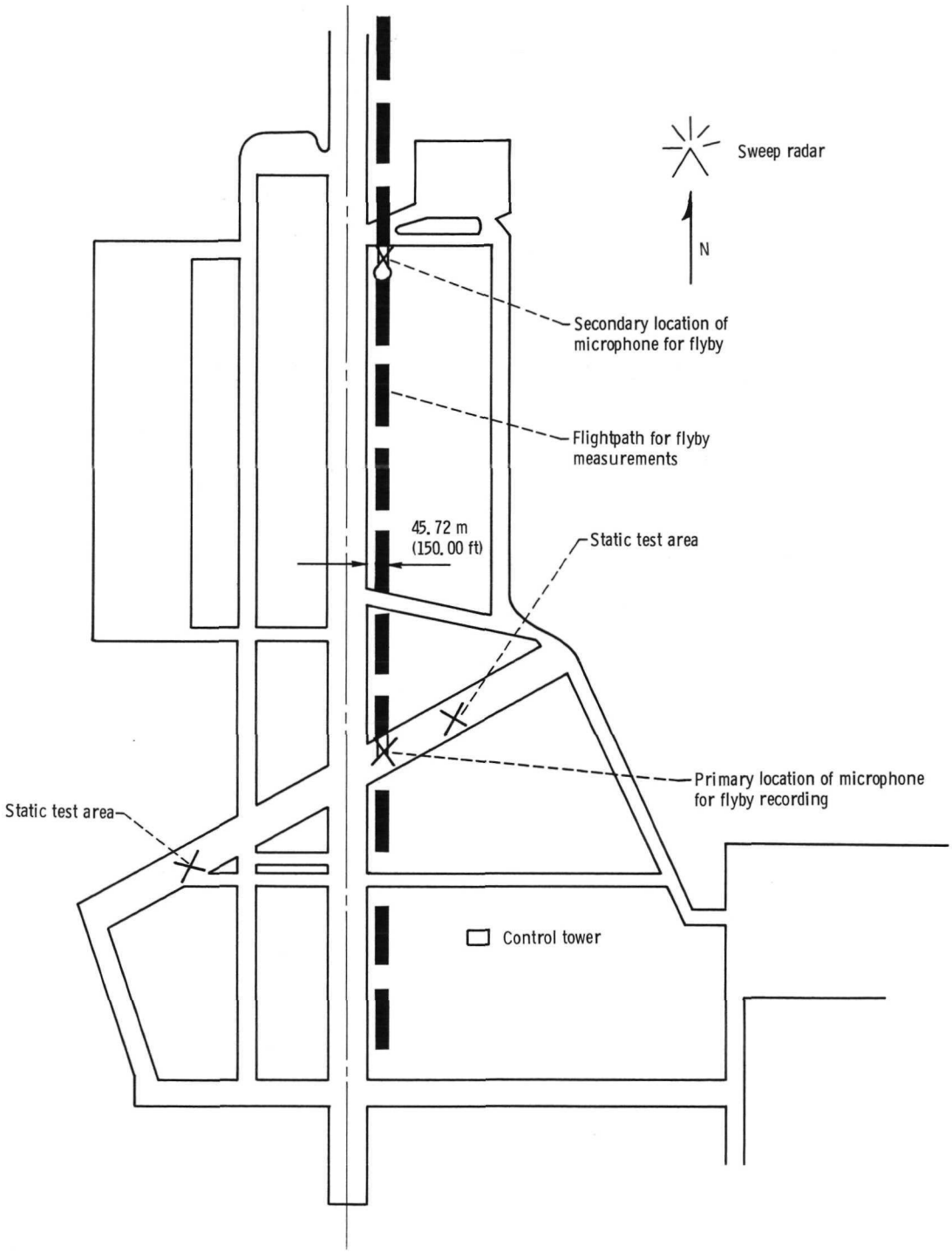

Figure 9. - Noise measurement locations at Selfridge Field.

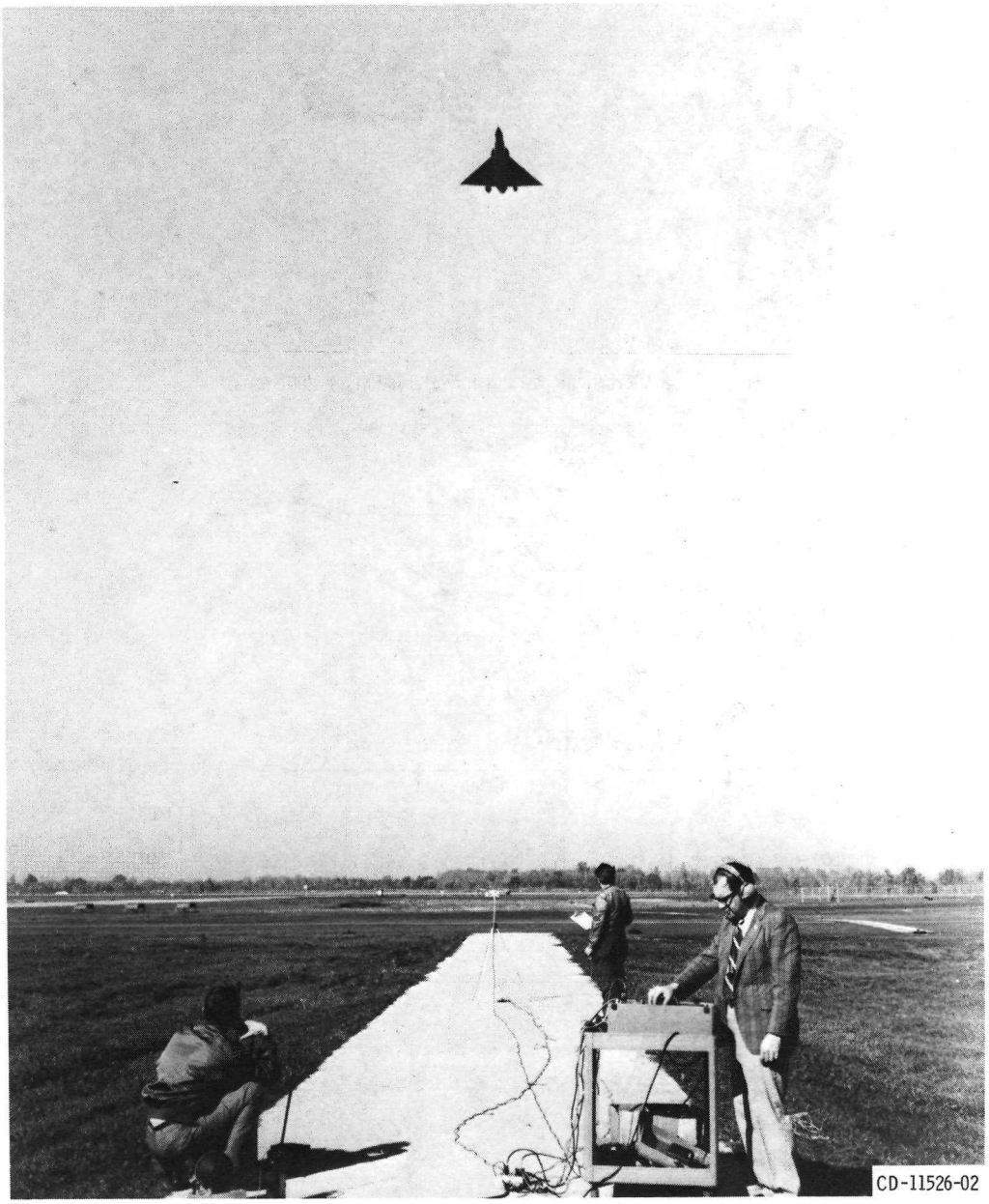

Figure 10. - Microphone position and orientation for flyover tests.

Figure 11. - Microphone position and orientation for static tests.

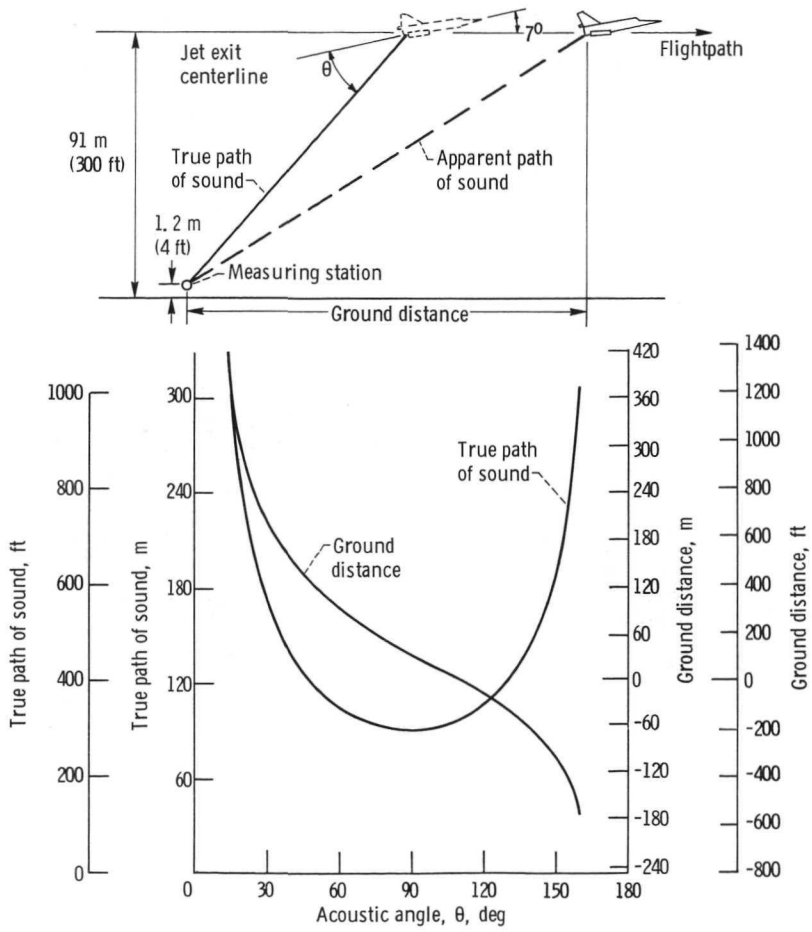

Figure 12. - Flyover geometry.

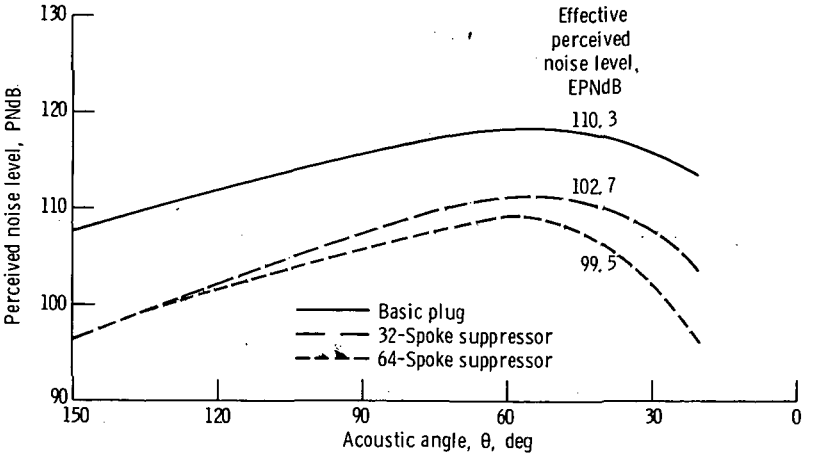

Figure 13. - Flyover noise levels directly beneath flightpath. Free-stream Mach number, 0.4; altitude, 91 meters (300 ft). Data adjusted to free-field, standard-day conditions; relative velocity, 543 meters per second (1780 ft/sec).

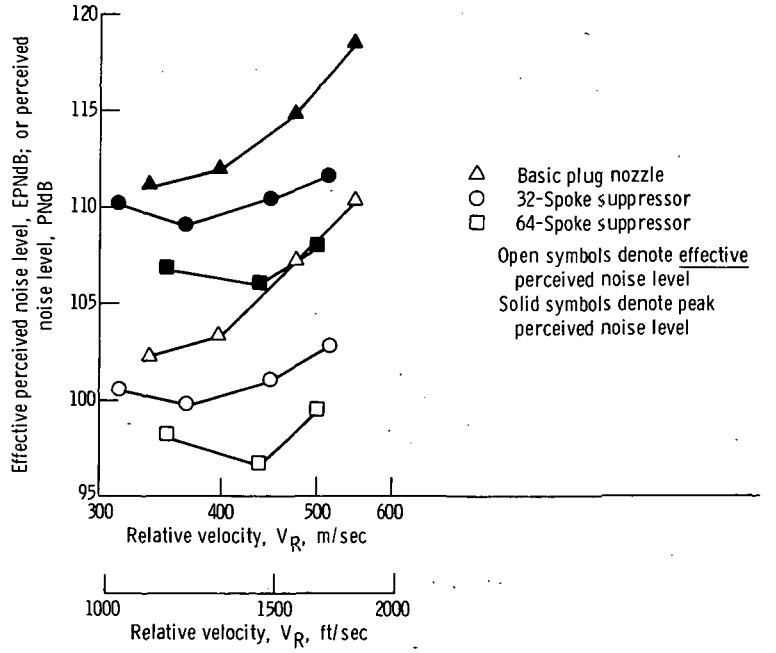

Figure 14. - Effective perceived noise level and peak perceived noise level under flightpath. Free-stream Mach number, 0.4; altitude, 91 meters (300 ft). Data adjusted to standard-day and free-field conditions.

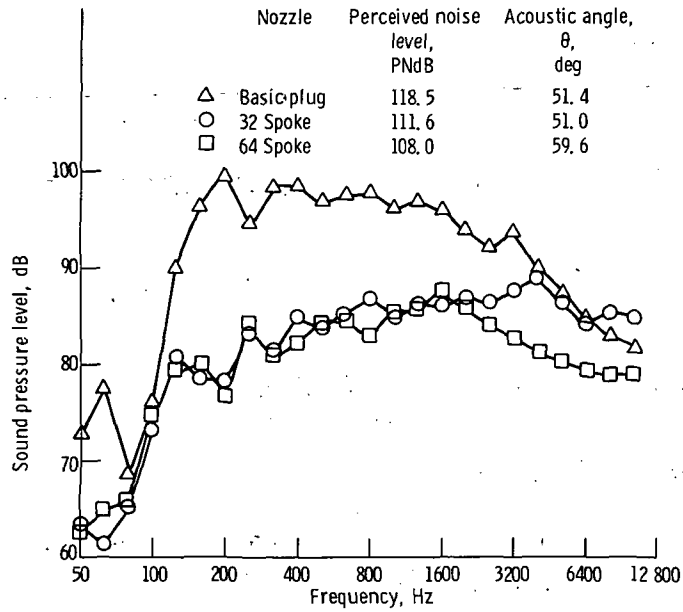

Figure 15. - Frequency spectra under flightpath. Free-stream Mach number, 0.4; altitude, 91 meters (300 ft). Peak PNL points adjusted to free-field and standard-day conditions.

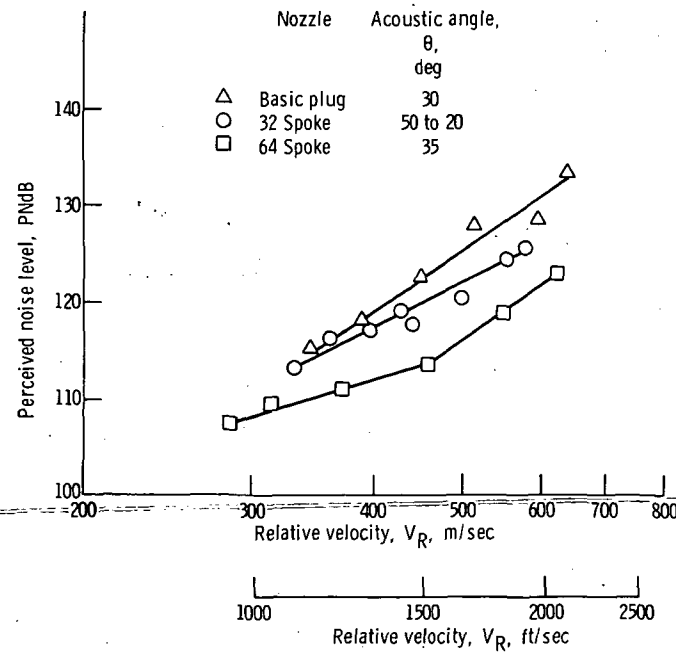

Figure 16. - Static peak perceived noise level at 30-meter (100-ft) radius adjusted to free-field and standard-day conditions.

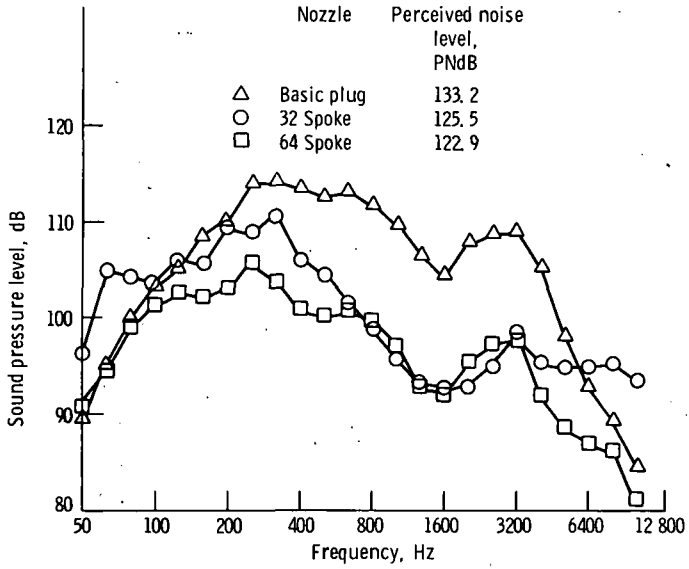

Figure 17. - Static frequency spectra at 30-meter (100-ft) radius. Peak PNL points adjusted to free-field and standard-day conditions.

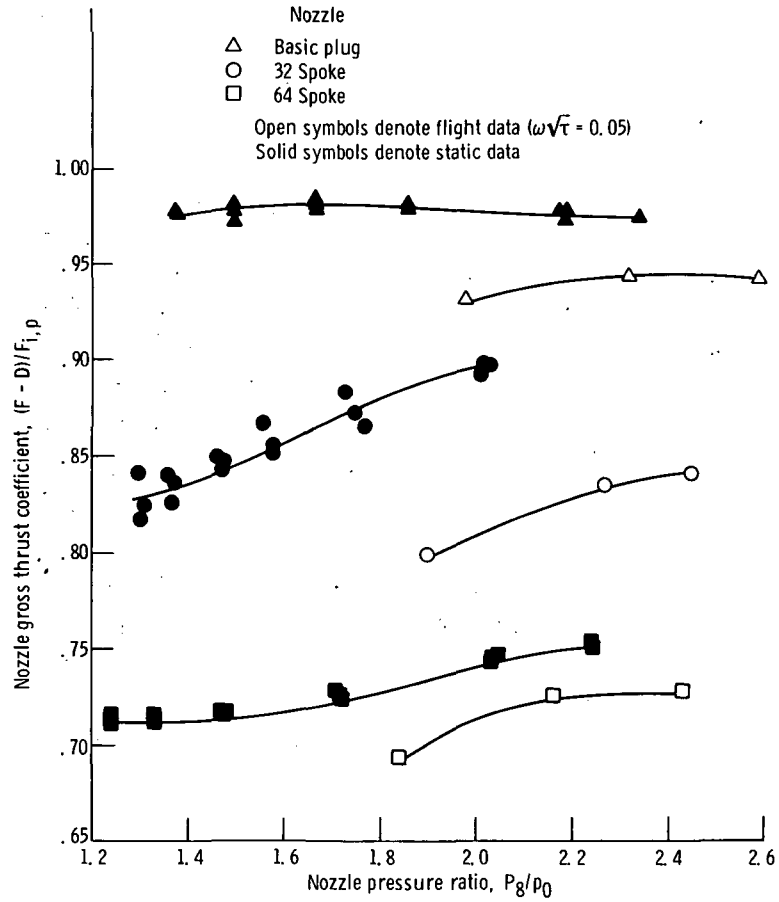

Figure 18. - Nozzle performance - static and flyby. Flight conditions: free-stream Mach number, 0.4; altitude, 91 meters (300 ft); corrected secondary weight flow ratio, 0.05.

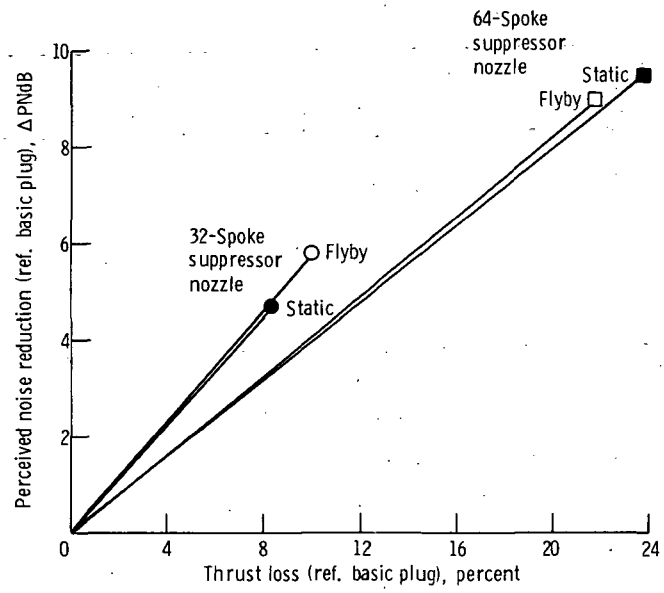

Figure 19. - Peak noise reduction as function of thrust loss - static and flyby. Flight conditions: relative velocity, V_R = 543 meters per second (1780 ft/sec); nozzle pressure ratio, P_8/p_0 = 2.4; altitude, 91 meters (300 ft). Static conditions: V_R = 600 meters per second (1970 ft/sec); P_8/p_0 = 2.0; microphone radius from aircraft, 30 meters (100 ft).

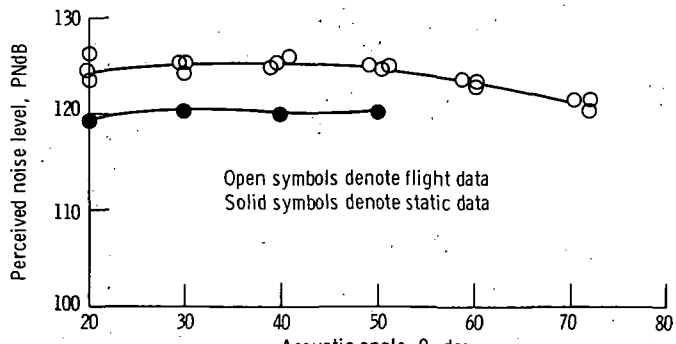

Figure 20. - Comparison of flight and static noise levels for 32-spoke nozzle. Both static and flight data adjusted to reference conditions. Relative velocity, V_R, meters per second (ft/sec): flight, 518 (1700); static, 503 (1650).

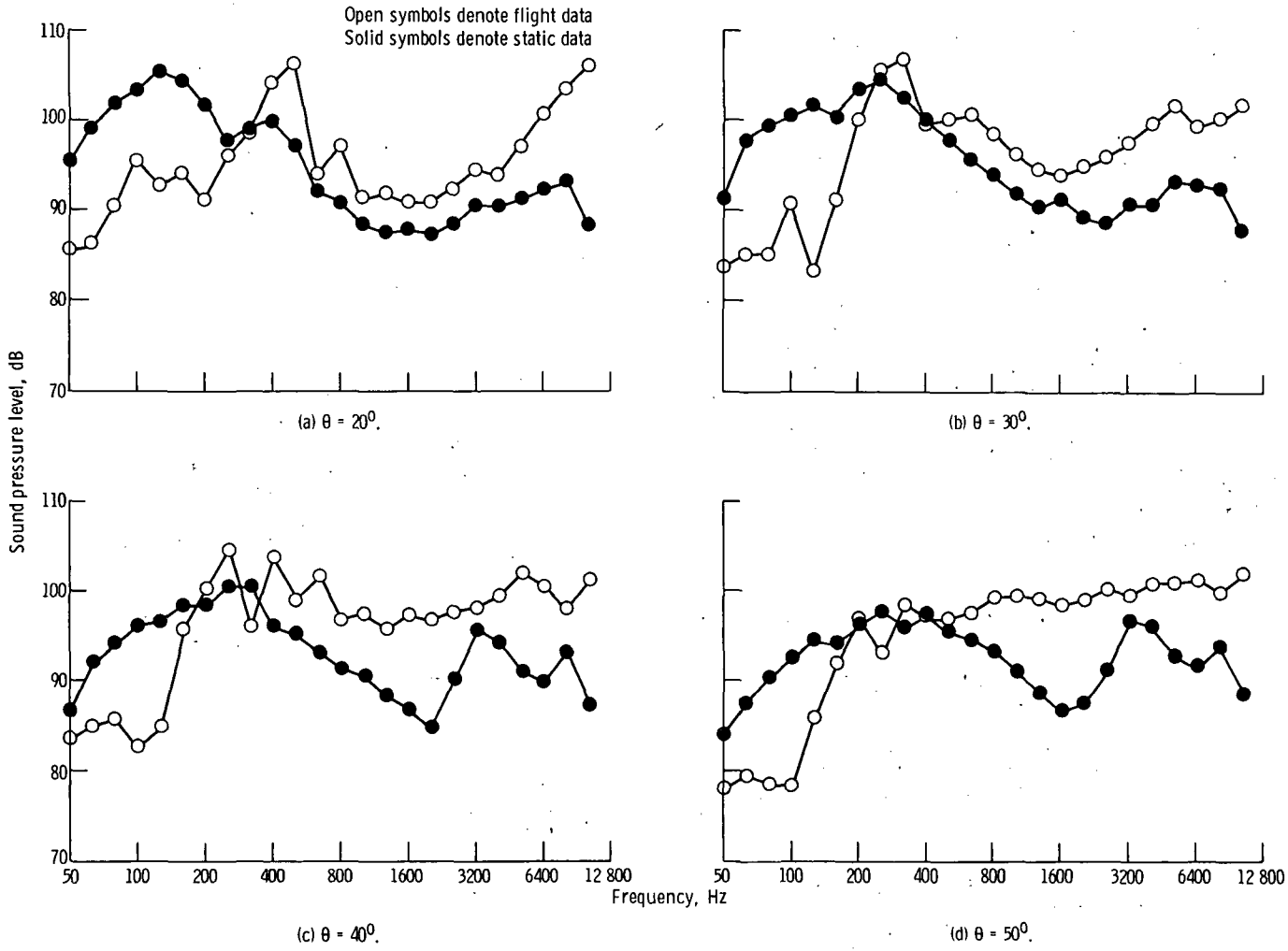

Figure 21. - Comparison of frequency spectra for 32-spoke nozzle - static and flyby - for various acoustic angles. Both static and flight data adjusted to reference conditions. Relative velocity, V_R, meters per second (ft/sec): flight, 518 (1700); static, 501 (1645).

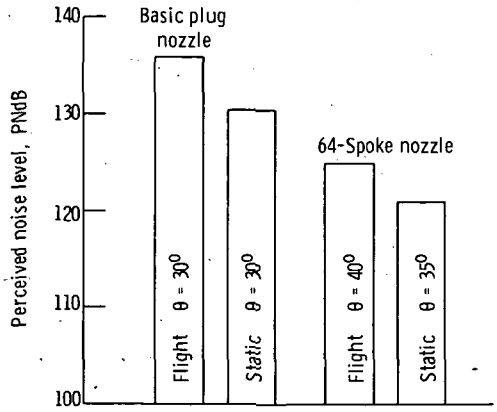

Figure 22. - Comparison of flight and static perceived noise. Both flight and static data adjusted to reference conditions and to a relative velocity V_R of 600 meters per second (1970 ft/sec).

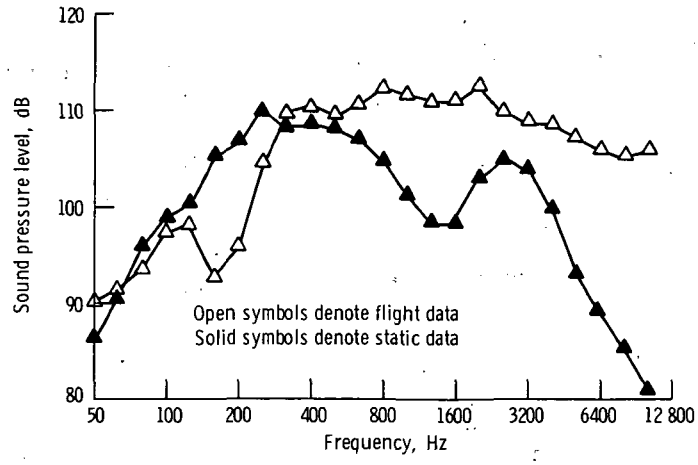

Figure 23. - Comparison of frequency spectra for the basic plug nozzle - static and flyby. Both static and flight data adjusted to reference conditions. Relative velocity, V_R, meters per second (ft/sec): flight, 558 (1831); static, 600 (1970), acoustic angle $\theta = 30^0$.

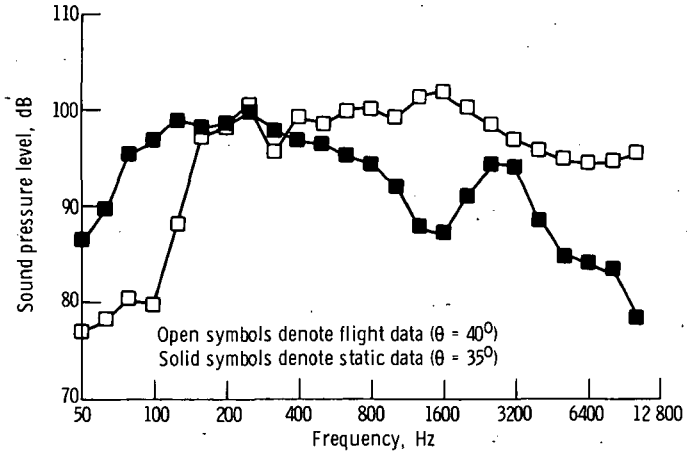

Figure 24. - Comparison of frequency spectra for the 64-spoke nozzle - static and flyby. Both static and flight data adjusted to reference conditions. Relative velocity, V_R, meters per second (ft/sec): flight, 526 (1726); static, 556 (1825).

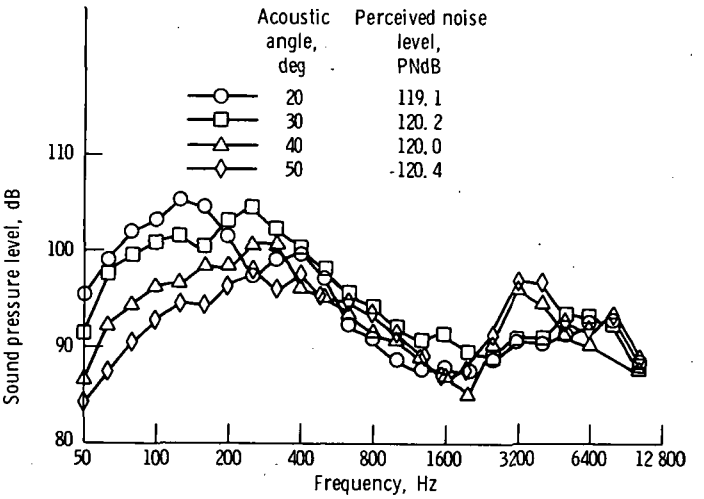

Figure 25. - Comparison of static frequency spectra for 32-spoke nozzle - for various acoustic angles. Data adjusted to reference conditions. Relative velocity, V_R = 501 meters per second (1645 ft/sec).

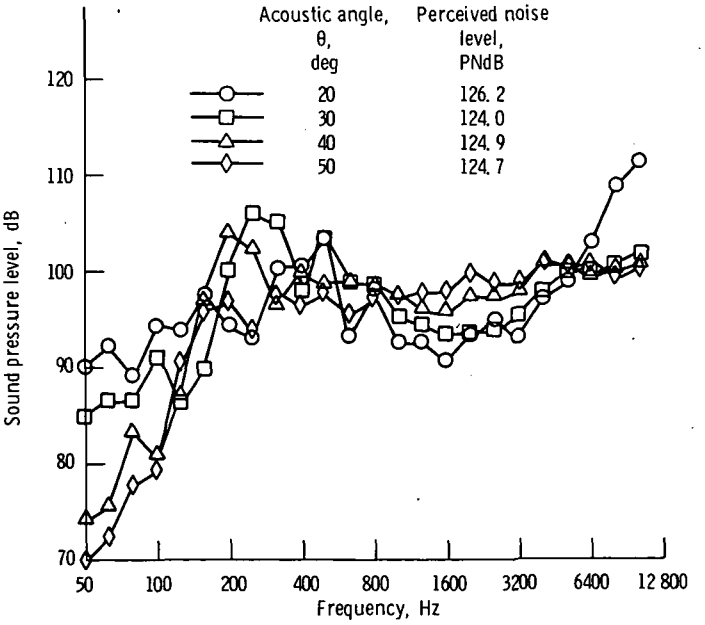

Figure 26. - Comparison of flight frequency spectra for 32-spoke nozzle - for various acoustic angles. Data adjusted to reference conditions. Relative velocity, V_R = 522 meters per second (1713 ft/sec).

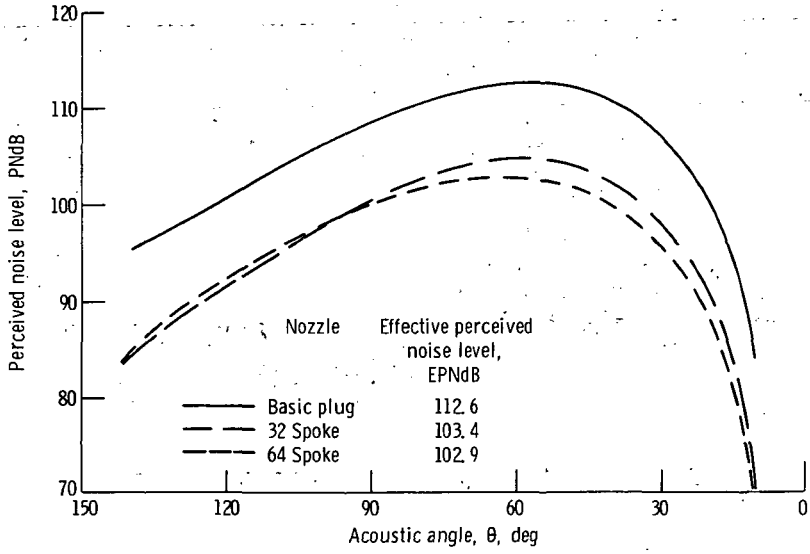

Figure 27. - Flight noise levels scaled to four large engines and adjusted to a 1.2-meter (4-ft) high microphone at a 640-meter (2100-ft) sideline distance. Relative velocity, $V_R \approx 533$ meters per second (1750 ft/sec).

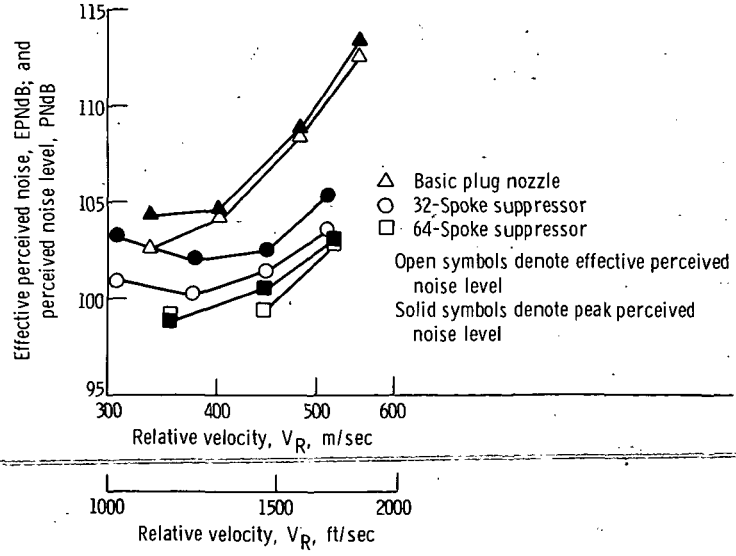

Figure 28. - Effective perceived noise level and peak perceived noise level. Flight data scaled to four large engines and adjusted to a 1.2-meter (4-ft) high microphone at a 640-meter (2100-ft) sideline distance.

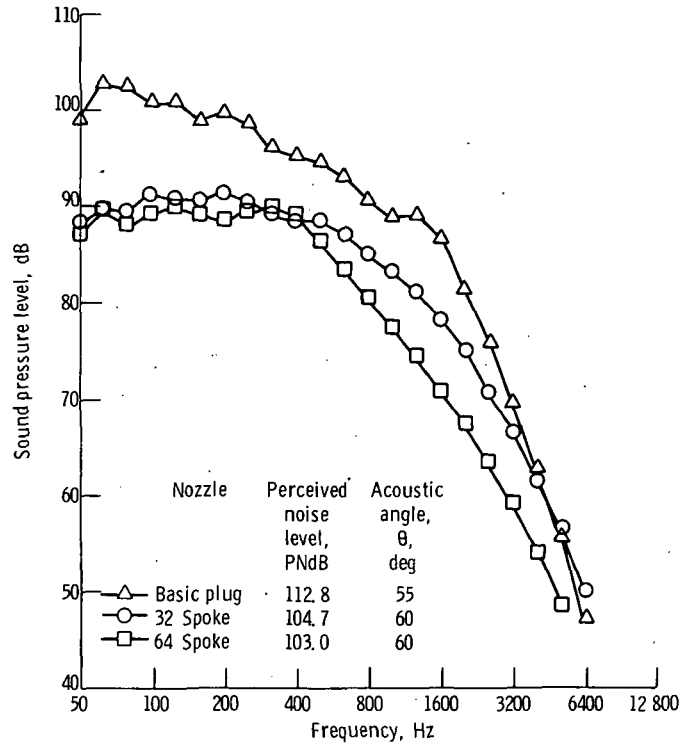

Figure 29. - Frequency spectra of flight data scaled to four large engines and adjusted to a 1.2-meter (4-ft) high microphone at a 640-meter (1200-ft) sideline distance. Relative velocity, V_R = 533 meters per second (1750 ft/sec).

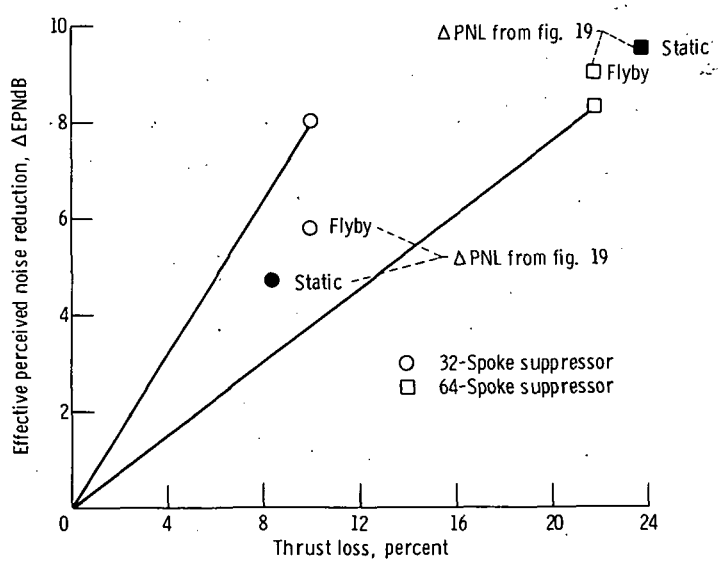

Figure 30. - Noise reduction as function of thrust loss (ref. basic plug nozzle). Flight data scaled to four large engines and adjusted to a 1.2-meter (4-ft) high microphone at a 640-meter (1200-ft) sideline distance. Relative velocity, V_R = 543 meters per second (1780 ft/sec).

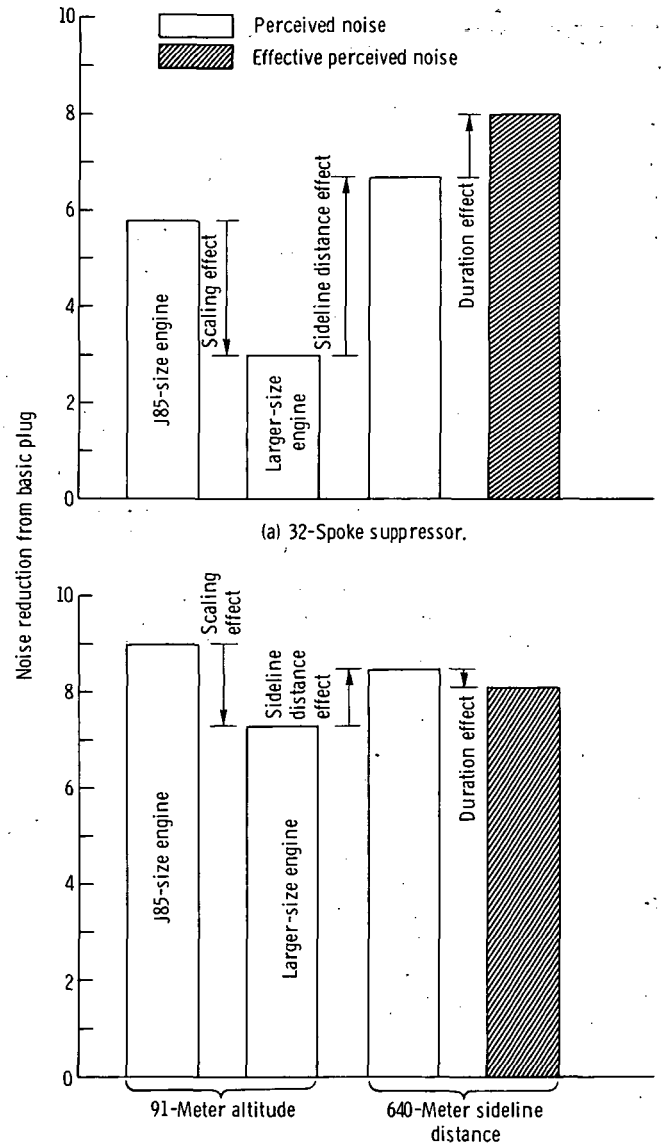

Figure 31. - Noise reductions associated with the different adjustments to scaled sideline conditions.

NASA-Langley, 1973 — 28 E-7186

Page Intentionally Left Blank

"The aeronautical and space activities of the United States shall be conducted so as to contribute . . . to the expansion of human knowledge of phenomena in the atmosphere and space. The Administration shall provide for the widest practicable and appropriate dissemination of information concerning its activities and the results thereof."

—NATIONAL AERONAUTICS AND SPACE ACT OF 1958

NASA SCIENTIFIC AND TECHNICAL PUBLICATIONS

TECHNICAL REPORTS: Scientific and technical information considered important, complete, and a lasting contribution to existing knowledge.

TECHNICAL NOTES: Information less broad in scope but nevertheless of importance as a contribution to existing knowledge.

TECHNICAL MEMORANDUMS: Information receiving limited distribution because of preliminary data, security classification, or other reasons. Also includes conference proceedings with either limited or unlimited distribution.

CONTRACTOR REPORTS: Scientific and technical information generated under a NASA contract or grant and considered an important contribution to existing knowledge.

TECHNICAL TRANSLATIONS: Information published in a foreign language considered to merit NASA distribution in English.

SPECIAL PUBLICATIONS: Information derived from or of value to NASA activities. Publications include final reports of major projects, monographs, data compilations, handbooks, sourcebooks, and special bibliographies.

TECHNOLOGY UTILIZATION PUBLICATIONS: Information on technology used by NASA that may be of particular interest in commercial and other non-aerospace applications. Publications include Tech Briefs, Technology Utilization Reports and Technology Surveys.

Details on the availability of these publications may be obtained from:

SCIENTIFIC AND TECHNICAL INFORMATION OFFICE

NATIONAL AERONAUTICS AND SPACE ADMINISTRATION

Washington, D.C. 20546